Modelling the response of Placentia Bay to hurricanes Igor and Leslie

Zhimin Ma [a,b], Guoqi Han [b,*], Brad de Young [a]

[a] *Department of Physics and Physical Oceanography, Memorial University of Newfoundland, St. John's, Newfoundland, Canada*
[b] *Biological and Physical Oceanography Section, Fisheries and Oceans Canada, Northwest Atlantic Fisheries Centre, St. John's, Newfoundland, Canada*

A R T I C L E   I N F O

A B S T R A C T

A three-dimensional, baroclinic, finite-volume ocean model (FVCOM) is used to examine hurricane induced responses in Placentia Bay, Newfoundland. Hurricane Igor (2010) and Hurricane Leslie (2012) made landfall within 100 km of the mouth of the bay, with the former to the eastern side and the latter on the western side. The model results have reasonable agreement with field observations on sea level, near-surface currents and sea surface temperature (SST). During landfall the two hurricanes cause the opposite shifts in inner bay circulation. Hurricane Igor overwhelms the mean inflow into the inner bay and shifts the currents to outflow. Hurricane Leslie reinforces the inflow into the inner bay. The peak storm surge is significantly influenced by local wind and air pressure during Leslie, accounting for 34% and 62% at the Argentia and St. Lawrence tide-gauge stations respectively, but predominately due to remote forcing entering the upstream eastern open boundary during Igor. There is a strong near-surface near-inertial response during Leslie, but a weak one during Igor. Stratification plays an important role in both generation and dissipation of near-inertial oscillation. A strong pre-storm stratification during Leslie favours the generation of near-inertia oscillation. Strong turbulent mixing induced on the right side of Leslie generates large vertical movement of the thermocline and thus contributes to strong near-inertia oscillation inside the mixed layer. The barotropic simulation results in a significant underestimation of near-surface currents and near-inertial oscillation. The baroclinic simulation shows a large increase of the current gradient in the vertical, as the first baroclinic mode in response to the hurricane forcing.

© 2017 Published by Elsevier Ltd.

1. Introduction

Placentia Bay is located in southern Newfoundland, bordered by the Burin Peninsula to the west and the Avalon Peninsula to the east. It supports important fisheries, especially for Atlantic Cod, which has received considerable interest recently because of its ecological sensitivity and economic importance (Bradbury et al., 2000). In summer, Placentia Bay features coastal upwelling on the western side of the bay due to the westerly upwelling favourable wind. The mean circulation of the bay is observed to be cyclonic (Hart et al., 1999; Shillinger et al., 2000) and is simulated by modelling studies (Greenberg and Petrie, 1988; Tang et al., 1996; Han, 2005; Han et al., 2008; Han et al., 2011; Ma et al., 2012). Ma et al. (2012) applied a robust prognostic high resolution model on Placentia Bay. They reproduced the mean circulation and modelled the spring-summer seasonal hydrographic variability in 1999. The Smart Bay project funded by the Marine Institute of Memorial University deployed three buoy stations in Placentia Bay to collect real-time near surface currents and temperature data. Occasionally

hit by tropical storms during late summer, the oceanic responses of the Grand Banks (Connecting Placentia Bay at its east end, see Fig. 1) to a moving hurricane is characterized by a rise in sea level, a decrease in sea surface temperature and a surface phytoplankton bloom (Han et al., 2012a). In recent years, Placentia Bay was hit by two major hurricanes, Hurricane Igor on 21 September 2010, considered to be the most intense hurricane to Newfoundland in recent years (Pasch and Kimberlain, 2011), and Leslie on 11 September 2012. Both hurricanes made landfall at southern Newfoundland (Table 1). Their tracks were almost parallel to each other and 45° northeast towards the coast (see black thick lines in Fig. 1). Igor made landfall to the east of Placentia Bay, classified as an eastern-type storm based on the landfall location, while Leslie's landfall was on the western side of Placentia Bay as a western-type storm. The storm translation speed intensifies the wind speed on the right side of storm and reshapes the storms, resulting in asymmetry. Leslie had its right side facing Placentia Bay and the landfall point is at the mouth of bay (Fig. 1 and Table 1). The eastern-type storm like Igor had the bay on its left side. The differences in tracks and landfall locations lead to significantly different oceanic responses in Placentia Bay.

---

* Corresponding author.
  E-mail address: guoqi.han@dfo-mpo.gc.ca (G. Han).
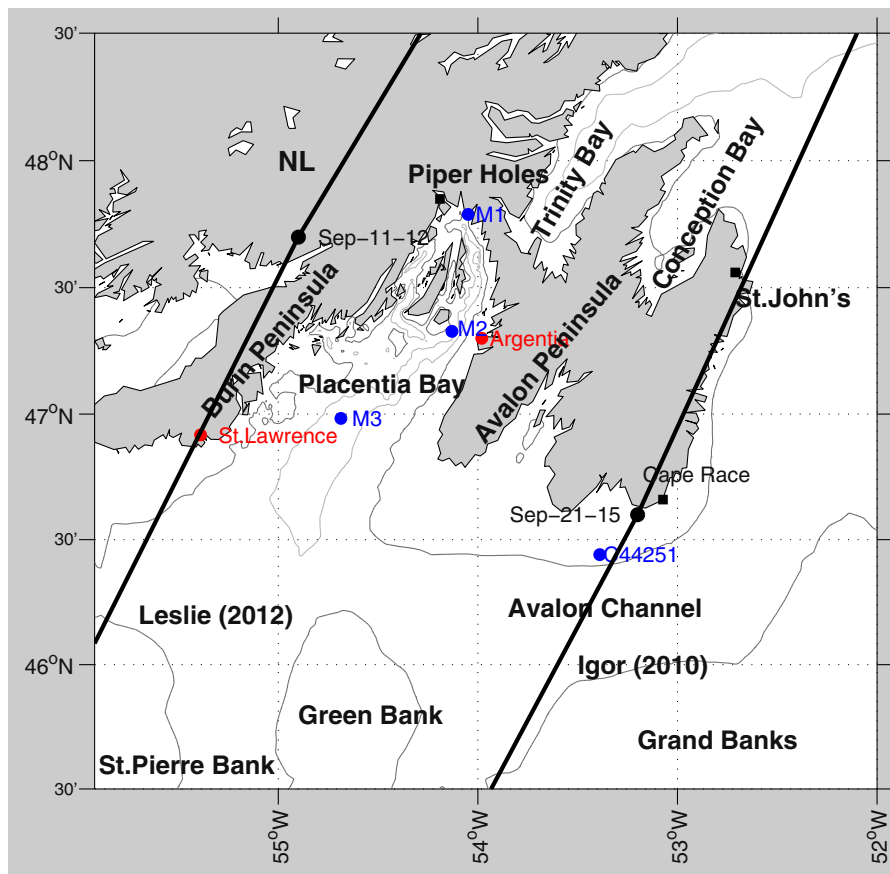
Fig. 1. Map showing model domain including 100 and 200 m depth contours (gray lines). Black thick lines are the tracks for Hurricane Igor and Hurricane Leslie. The red dots are tide-gauge stations, and the blue dots indicate mooring stations for surface temperature and currents. NL: Newfoundland. (For interpretation of the references to colour in this figure legend, the reader is referred to the web version of this article.)

Table 1
Some comparative aspects of Hurricane Igor and Leslie.

| Name	Hurricane Igor	Hurricane Leslie
Date under effect	September 21–22, 2010	September 11–12, 2012
Landfall location	Burin Peninsula, Newfoundland (East)	Cape Race, Newfoundland (South)
Maximum sustainable wind	40 m s^{-1}	35 m s^{-1}
Minimum centre pressure	950 mb	968 mb
Peak storm surge at Argentia	0.85 m	1.02 m
Peak storm surge at St. Lawrence	0.74 m	0.90 m
Distance from landfall point to mouth of Placentia Bay	Around 100 km	0 km

In this paper, we investigate oceanic responses of Placentia Bay to Hurricane Igor and Leslie using a three-dimensional (3-D), coastal ocean model (FVCOM, Chen et al., 2004). Our main objectives are to validate the model against independent observational data including mooring and tide-gauge data, to study the oceanic responses of Placentia Bay to both hurricanes and their differences and to examine the importance of baroclinicity in the oceanic responses.

This paper is arranged as follows. In Section 2, we will describe the model setup, boundary conditions, forcing data and initial conditions. In Section 3, we will evaluate model results against observations. In Section 4, we will examine circulation variability during Hurricane Igor and Leslie, as well as the relative importance of local wind in generating peak storm surges. Then we will investigate near-inertial oscillation and the importance of stratification. Finally, in Section 5, we will present the summary and conclusions.

2. Model configuration

2.1. FVCOM model (Version 3.1)

Combining horizontal grid flexibility and computational efficiency, the FVCOM model used in this study integrates independent variables through individual unit control volumes. It is solved numerically by flux through the volume boundaries to guarantee the horizontal conservation of mass and momentum. A time splitting method is used for computational efficiency including an internal mode and an external mode constrained by the Courant-Friedriches-Levy (CFL) condition. A sigma coordinate is chosen to better resolve the topography. Barometric pressure term is applied in momentum equations. Previous work (Weisberg and Zheng, 2006; Resio and Westerink, 2008; Rego and Li, 2010; Han et al., 2011; Ma et al., 2012; Ma et al., 2015) successfully demonstrates the advantage of FVCOM in simulating the physical environment on coastal shelves and embayments.
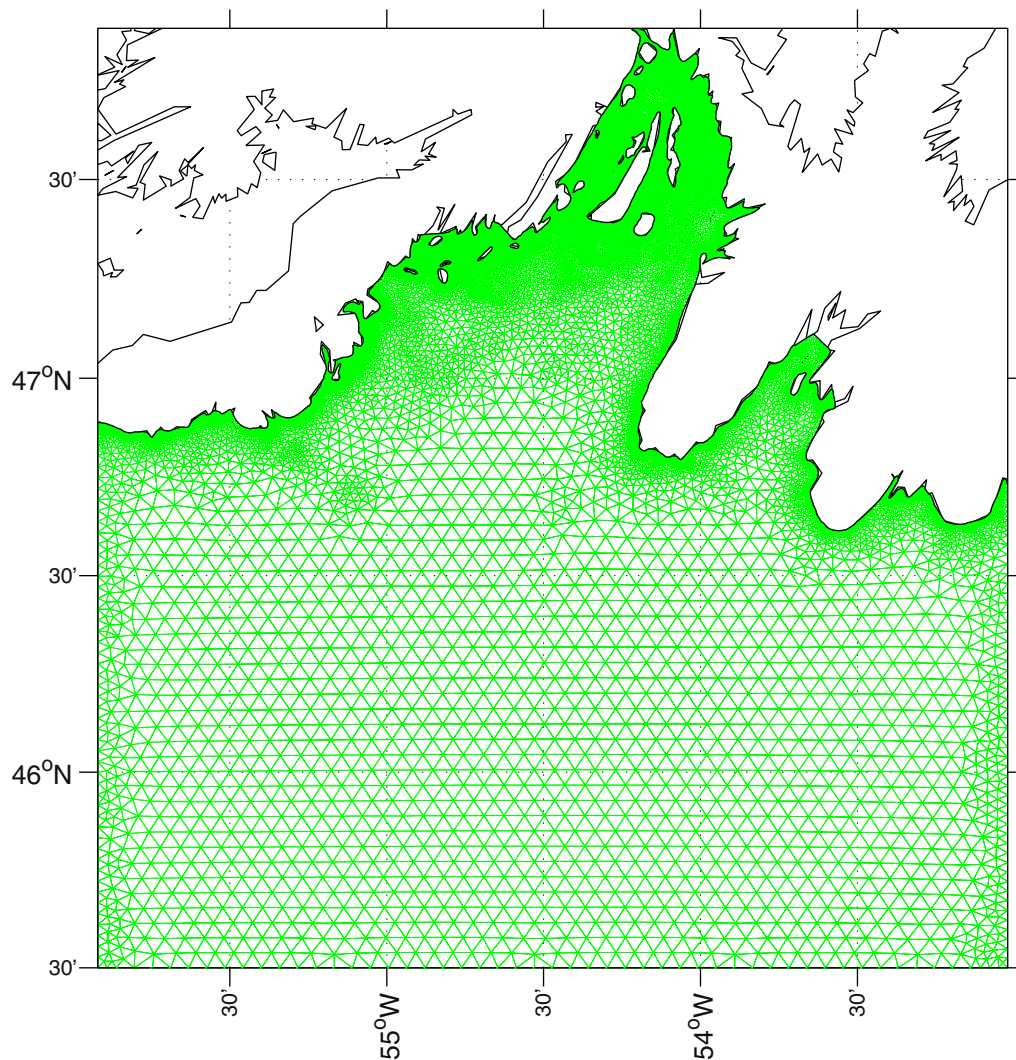
Fig. 2. The horizontal grid used in the numerical model. The grid spacing ranges from 50 m in the inner Bay to 5 km in the outer Bay.

2.2. Model domain

The shoreline of Placentia Bay has many inlets, and is surrounded by relatively steep cliffs. Three large islands are located in the inner portion of Placentia Bay (Fig. 1) and there are 400 m deep channels that run along the longitudinal axis of the inner bay. The centre of the outer bay is 200 m deep, while much of the remainder is typically 100 m deep. The model domain is shown in Fig. 2, covered with green irregular triangular grids. The model bathymetry is mainly derived from the multi-beam bathymetry of the Canadian Hydrographic Service. To minimize the pressure gradient errors (Mellor et al., 1993), the bathymetry was smoothed using the same method as in Foreman et al. (2009) and Ma et al. (2012). The governing equations of the model are solved on an unstructured triangular grid whose spacing is largest (3–5 km) along the open boundary and smallest (50 m) over the inner bay (Fig. 2). There are 31 unequally spaced levels in the vertical, with a minimum spacing of within 0.2 m near sea surface and seabed in order to resolve the shear current and thermodynamic process near surface and bottom. The model equations are solved using an integration step of 0.5 s for the external mode and an internal to external mode ratio of 10. The $k - \varepsilon$ turbulence model from GOTM (http://www.gotm.net/) is used as a default turbulence scheme.

2.3. Model forcing and initial conditions

The model is forced by winds, air pressure and heat fluxes at the sea surface, tidal and non-tidal sea levels as well as temperature and salinity at the lateral open boundaries. Wind and air pressure fields from Ma et al. (2015) are interpolated onto the model grids. These fields are blended from 3 hourly North American Regional Reanalysis (NARR) atmospheric forcing (www.esrl.noaa.gov/psd) and hourly Holland hurricane model (Holland, 1980). The blending method is described in Ma et al. (2015). To improve the accuracy of the wind and air pressure fields, a distance-weighted correction scheme (Shen et al., 2006) based on the observed atmospheric data is applied. This scheme uses the observed wind speed, direction and air pressure from local weather stations in the bay (See Fig. 1 for locations of M1, M2 and M3 from the Smart Bay Project; C44251 from Environment Canada; Argentia and St. Lawrence from Environment Canada) to correct the blended wind and air pressure fields. Net shortwave flux is extracted from NARR dataset (www.esrl.noaa.gov/psd, Mesinger et al., 2006) over the entire computational domain. The NARR is an extension of the NCEP Global Reanalysis that is run over North America. This dataset has output 8 times daily with a resolution of approximately 0.3°. Net longwave, latent and sensible fluxes are calculated based on the Argentia weather station from the
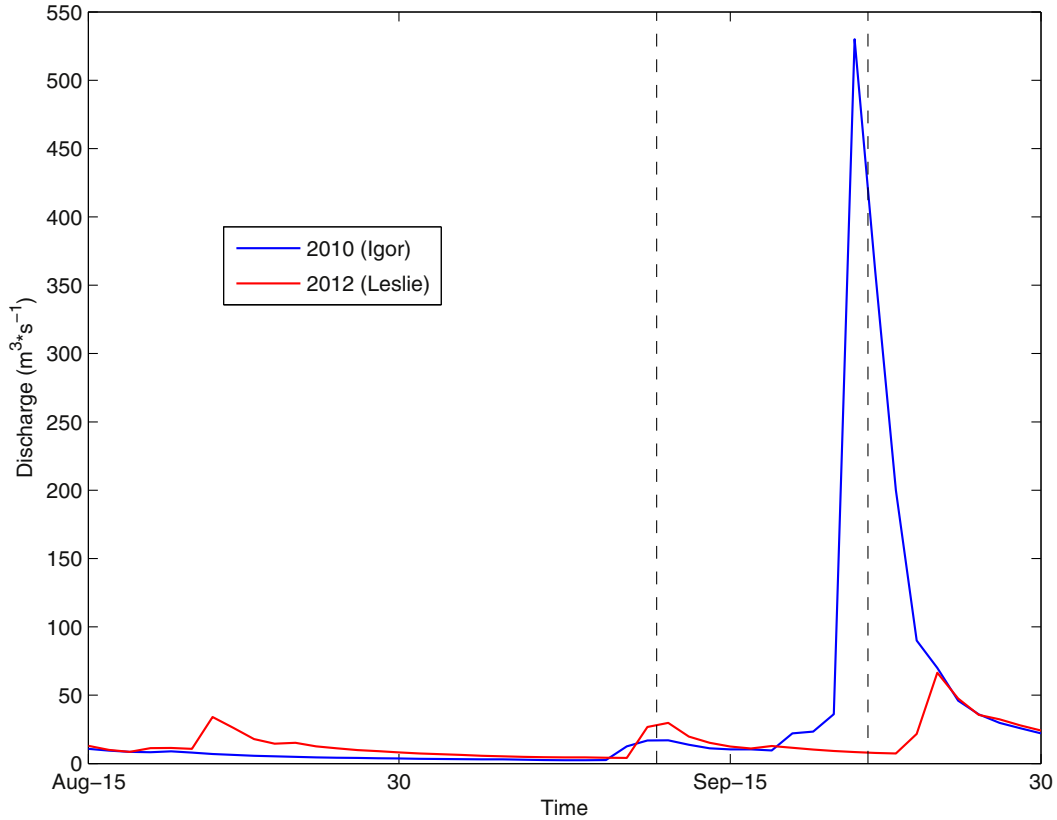
Fig. 3. Time series of Piper Holes River discharges in 2010 (blue) and 2012 (red). The black dashed lines indicate the landfall time at 15:00 21 September 2010 (Igor) and 10:45 11 September 2012 (Leslie). (For interpretation of the references to colour in this figure legend, the reader is referred to the web version of this article.)

air-sea toolbox developed by Bob Beardsley and Rich Pawlowicz (http://woodshole.er.usgs.gov/operations/sea-mat/), and are therefore uniform in the model domain. Five leading semidiurnal and diurnal constituents (M_2,S_2,N_2,K_1,O_1) and non-tidal sea levels at the lateral open boundaries are obtained from a large-scale Newfoundland Shelf model (Ma et al., 2015) and specified along the open boundaries. Experiments showed a non-tidal sea level difference between model east coastal open boundary and the average of Argentia and St. John's. This difference is added onto the open boundaries to provide better upstream dynamics. The hourly temperature and salinity along the open boundaries are specified based on the largescale shelf model as well. To maintain conservation, this condition is used only when the boundary flux is directed into the domain.

The sea level and velocity are initialized with the results of the large-scale Newfoundland Shelf model (Ma et al., 2015) throughout the computational domain to reduce the spin-up time. The initial temperature and salinity condition is also generated from the same source.

The present model considers the daily fresh water input from the Piper Holes River in the upper bay (see its location in Fig. 1). The linearly interpolated fresh water flux is applied every time step. The averaged river discharge rate during the model simulation period was 37 m³ s⁻¹ for 2010 and 15 m³ s⁻¹ for 2012. The maximum discharges of 530 m³ s⁻¹ occurred during Igor (Fig. 3).

The model is run from 15 August to 30 September in 2010 and 2012. Model results from 1 to 30 September are compared with observations and used in analysis. Based on previous work (Ma et al., 2012), 15 days are enough to spin up the model.

3. Validation

To evaluate the model solutions qualitatively and quantitatively, we compare the model solutions with various measurements. In addition to the correlation coefficient (R) and the root-mean-square (RMS) difference, we examine the velocity difference ratio (VDR) defined as the ratio of the sum of the squared magnitudes of the vector velocity differences to the sum of the squared magnitudes of the observed velocities, that is,

$$\text{VDR} = \sum |V_m - V_o|^2 / \sum |V_o|^2 \qquad (1)$$

where V_m is the horizontal model velocity and V_o is the horizontal observational velocity, lower VDR values indicate better agreement, with VDR=0 indicating exact agreement.

Another measure is the speed difference ratio (SDR) defined as the ratio of the sum of the squared speed difference to the sum of the squared magnitudes of the observed velocities, that is,

$$\text{SDR} = \sum (|V_m| - |V_o|)^2 / \sum |V_o|^2 \qquad (2)$$

3.1. Validation of non-tidal water levels

Hourly non-tidal water levels at Argentia and St. Lawrence are compared between the observations and the model results. Observed water levels are detided with the T-Tide toolbox (Pawlowicz et al., 2002). Harmonic analysis including five main tidal constituents (M_2, S_2, N_2, K_1, O_1) and major over-tides (M_4, M_6, MS_4) is applied to the model solutions. It should be noted observations are not available from 8 to 10 September 2012. Tidal currents are weak in Placentia Bay and their distributions have been studied in Ma et al. (2012). Tides are therefore considered as a minor part in this paper and have been excluded.
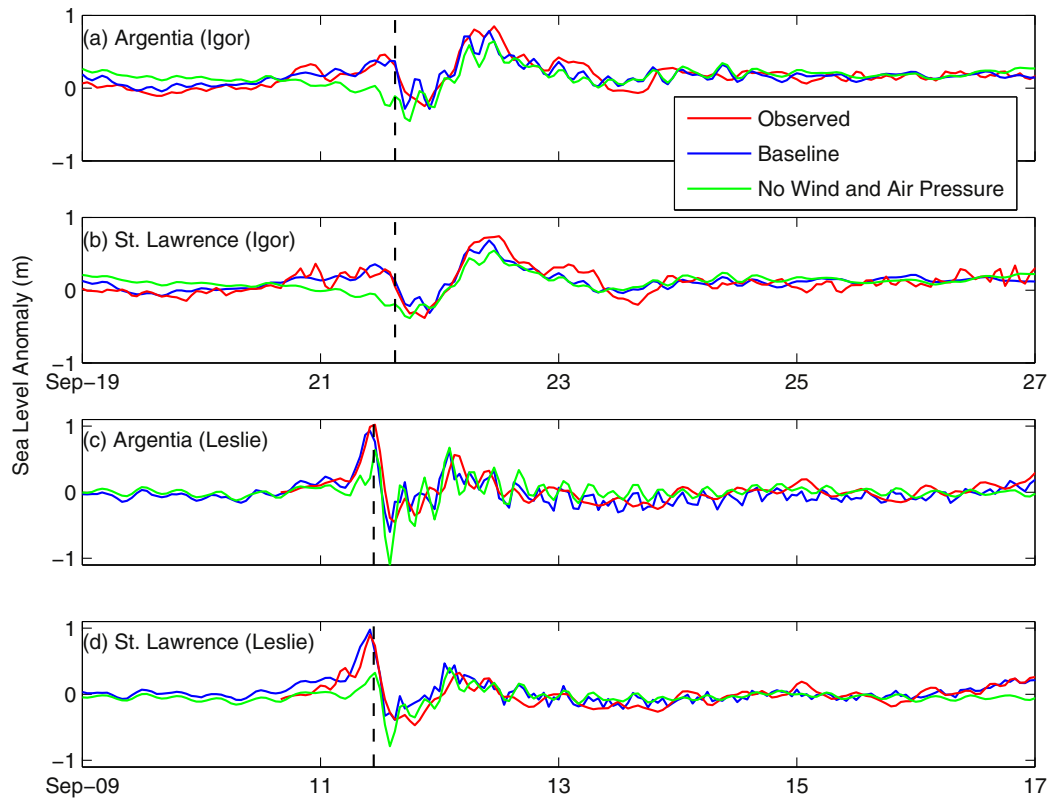
Fig. 4. Time series of de-tided sea level from tide-gauge observations, model with all forcing and model without wind and air pressure. Black dashed line indicates the landfall time at 15:00 21 September 2010 for Hurricane Igor and 10:45 11 September 2012 for Hurricane Leslie. (For interpretation of the references to color in the figure legend, the reader is referred to the web version of this article).

The model-data comparison is shown in Fig. 4 after we match model mean sea level to tide-gauge datum. Simulated water level responses to Igor agree well with observed ones at tide-gauge stations (Fig. 4a and b). Water levels showed the first peak at 13:00 pm 21 September when the storm centre made landfall near Cape Race (Southeast corner of the Newfoundland, Fig. 1). Around 21 hours later, a much higher peak developed at 10:00 am, 22 September as the storm centre travelled farther north to the central Labrador Sea. The storm surges during Igor have been discussed observationally and numerically in detail (Han et al., 2012b; Ma et al., 2015). Unlike Igor, the water levels associated with Leslie reached their peaks just before the storm made landfall at 10:45 am 11 September, 2012. Sea level at the tide-gauge stations started increasing from 10 September, until landfall (Fig. 4c and d). After peaking, sea level started to decrease and fluctuated for four cycles in one day with a period of about 5 h. This fluctuation could be attributed to seiches generated within Placentia Bay. The length of the bay is 130 km long, with an averaged depth of 120 m at the bay mouth. The fundamental seiche period is estimated to vary from 4.2 to 4.6 h depending on how we approximate bay's geometric shape (Rabinovich, 2009).

Quantitative comparisons are also made between the model results and observations (Table 2). By using the RMS difference and correlation, statistics are estimated to determine the model's ability to reproduce sea level variability under hurricane forcing. The averaged RMS difference and correlation coefficient for all the comparisons under both hurricanes are 0.09 m and 0.76, demonstrating reasonable agreement in terms of magnitude and variability. To evaluate the performance of the model in producing storm surge, the differences in surge magnitude and timing are calculated. On average, the absolute magnitude difference is 0.07 m and the absolute time difference is 1.0 h.

Table 2
Statistics for observed and modelled sea level anomalies at Argentia and St. Lawrence. See Fig. 1 for locations. (Model-Observation).

	Hurricane Igor		Hurricane Leslie	
	Argentia	St. Lawrence	Argentia	St. Lawrence
RMS difference (m)	0.08	0.08	0.10	0.11
Correlation	0.78	0.78	0.73	0.75
Surge difference (m)	−0.06	−0.06	−0.09	0.08
Surge time lag (h)	−1	−2	−1	0

3.2. Evaluation of non-tidal surface current

Model currents are evaluated with the buoy data from the Smart Bay Project (http://www.smartatlantic.ca/PlacentiaBay/). Current data at 0.5 m below sea surface were recorded every half hour at three different locations since 2006 (See locations of M1, M2 and M3 in Fig. 1). Currents at these different sites are likely to have quite different dynamical characteristics (Fig. 5). The surface current at M1 is relatively weak even during hurricanes (Fig. 5e and f) due to its location near the head of bay and its reduced influence from outside of the bay. At M3, Igor and Leslie resulted in opposite near-surface responses at the time of storm landfall, with southwestward currents under Igor (Fig. 5c and d) but strong northeastward currents under Leslie (Fig. 5g and h). The inertial period at M3 is 16.4 h. Currents fluctuate at a period of 16 h, suggesting a near-inertial oscillation (NIO) at M3 with increased inertial frequency described as blue-shifted (Kundu, 1976, 1985; Perkins, 1976; Mayer et al., 1981). The near-surface NIO is strong during Leslie in responding to direct and more energetic wind impact from the right side of Leslie (Price, 1981; Greatbatch, 1983) and is weak during Igor (further discussed in Section 4). Model
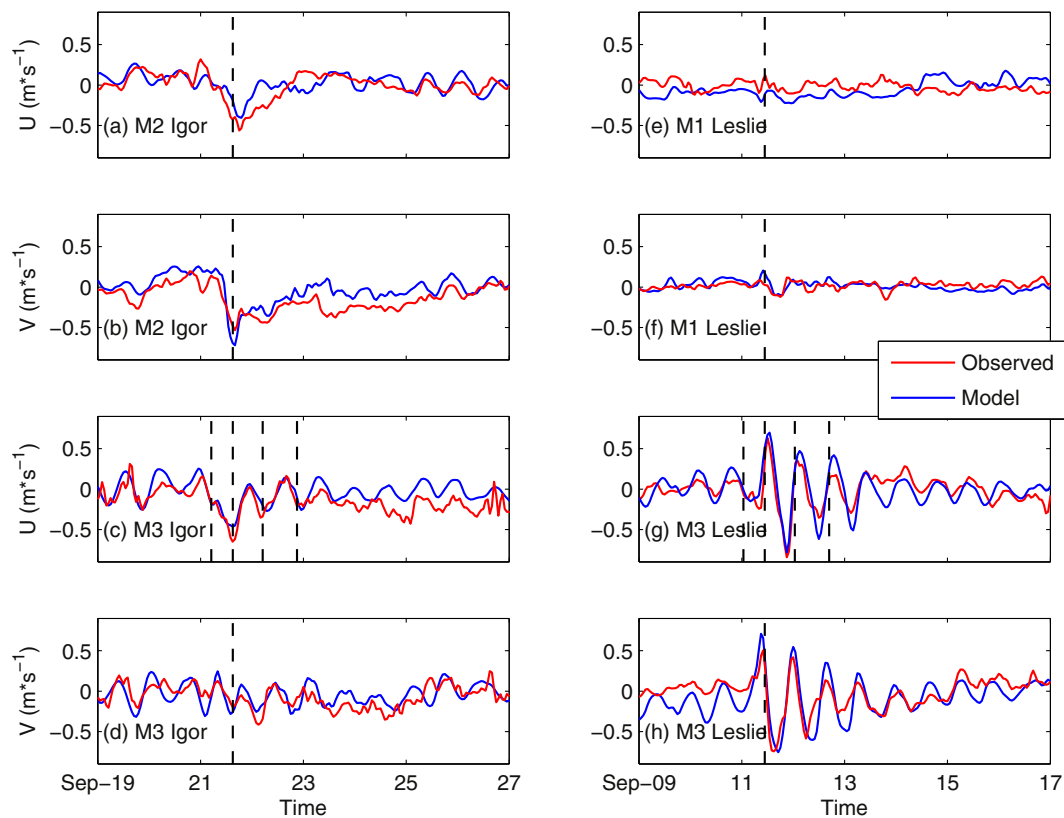
Fig. 5. Time series of de-tided observed and modelled near-surface current during Hurricane Igor and Leslie. Black dashed line indicates the landfall time at 15:00 21 September 2010 for Hurricane Igor and 10:45 11 September 2012 for Hurricane Leslie. Four black dashed lines at (c) and (g) mark the time at which the near-inertial speed is shown in Figs. 8 and 9. (For interpretation of the references to color in the figure legend, the reader is referred to the web version of this article).

Table 3
Current statistics for Eastward (U) and Northward (V) VDR and SDR at near surface for M1, M2 and M3. See Fig. 1 for the locations of M1, M2 and M3.

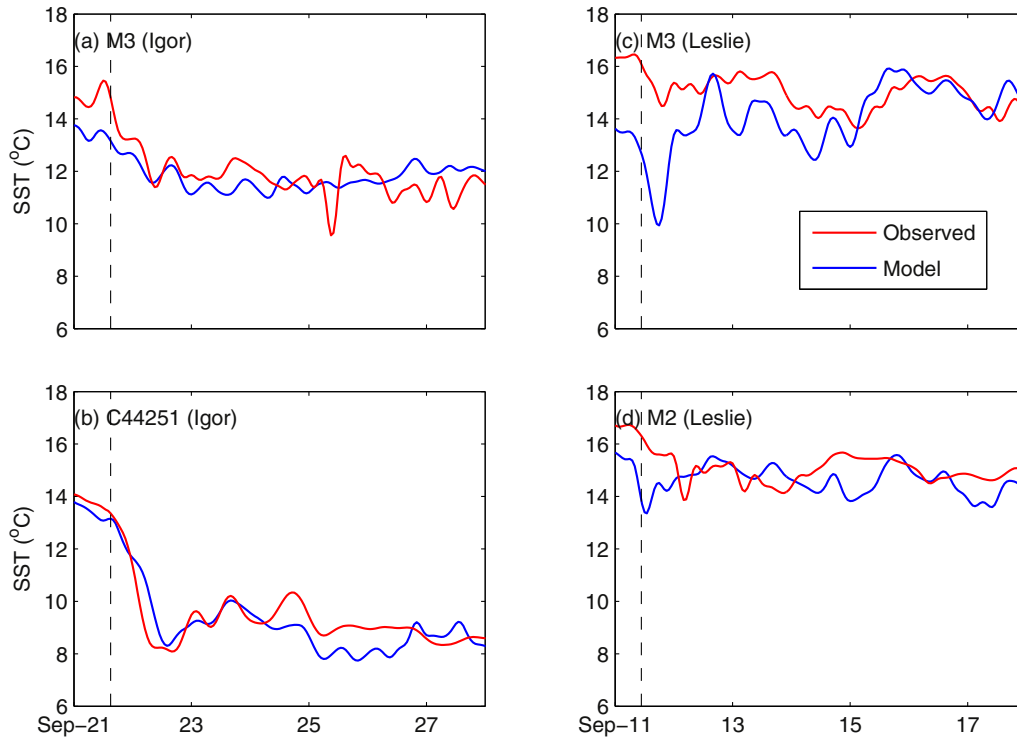|	Hurricane Igor				Hurricane Leslie			
	VDR	SDR	Correlation		VDR	SDR	Correlation	
			U	V			U	V
M1	–	–	–	–	3.2	0.8	−0.3	0.3
M2	0.6	0.2	0.7	0.8	–	–	–	–
M3	0.6	0.3	0.7	0.6	0.6	0.3	0.8	0.8

Table 4
Statistics for the comparison between modelled and observed sea surface temperature at C44251, M2 and M3. See Fig. 1 for the locations.

	Hurricane Igor		Hurricane Leslie	
	M3	C44251	M2	M3
RMS difference (°C)	1.3	1.0	1.2	1.4
Correlation	0.88	0.96	0.76	0.64

model and observations. The large VDR value at M1 is primarily due to the weak current magnitude there.

3.3. Comparison of sea surface temperature (SST)

Fig. 6 presents time series of surface temperature at M2, M3 and C44251 based on observations and model results for Hurricanes Igor and Leslie. The observed sea surface temperature at C44251 shows a sharp drop of 6 °C during Igor (Fig. 6b). The model temperature drop is also 6 °C at C44251, which is an improvement over the baseline case from Ma et al. (2015) shelf model having a temperature drop of 8 °C. At M3, the model sea surface temperature has a 3 °C decrease from 21 to 23 September (Fig. 6a), underestimating by 1.5 °C. Unlike Igor, the response to Hurricane Leslie shows weaker changes in surface temperature, with a ∼2 °C drop in sea surface temperature at M3 and M2 as the storm passed by (Fig. 6c and d). Simulated surface temperature under Leslie reproduces approximately the observed temperature drop. The RMS difference and correlation coefficient are calculated to quantify the model performance (Table 4). The RMS differences are less than 2 °C, indicating fair agreement between the model and observations.

results at M3 are well compared with observations in magnitude and phase during both hurricanes. Currents at M2 show large shifts in magnitude and direction during Hurricane Igor, without apparent near-inertial oscillation (Fig. 5a and b). The maximum southwestward current reached 0.6 m/s when Igor made landfall. The model does well at capturing observational variability and magnitude. Both observed and modelled currents at M1 show weak responses to Hurricane Leslie. The spatial difference of the near-surface currents at these three locations largely depends on the coastal geometry and the Rossby number.

Quantitative statistics are calculated between the model results and observations (Table 3). Data were unavailable at M1 during Igor and at M2 during Leslie. The correlation coefficients are greater than 0.5 at M2 and M3. The SDR values are smaller than 0.5 except for M1, indicating that the model is able to well simulate current magnitude in the outer bay. The VDR values, accounting for both speed and direction, are generally greater than SDR. All VDR estimates except for M1 indicate fair agreement between

Fig. 6. Time series of observed (red) and model results (blue) sea surface temperature (SST) at (a) M3 and (b) C44251 under Hurricane Igor; and SST at (c) M3 and (d) M2 under Hurricane Leslie. Black dashed line indicates the landfall time at 15:00 21 September 2010 and 10:45 11 September 2012. (For interpretation of the references to colour in this figure legend, the reader is referred to the web version of this article.)

4. Discussion

4.1. Circulation change before and during landfall

The time sequences of sub-tidal 0–30 m averaged flows related to Hurricane Igor and Leslie are shown in Fig. 7. On 10:00 am 21 September, around 5 h before the landfall of Igor, the upper-layer ocean current has an inflow through the eastern side of the steep channel into the inner bay (Fig. 7a). After Igor made landfall, the hurricane wind effect completely changes the surface circulation pattern (Fig. 7b). The upper-layer current becomes toward the southwest. At M2, the surface current is about 40° to the right of the wind direction. The current rotates anti-cyclonically about 50° and decrease in magnitude as the depth increases to 30 m. As Igor moves farther northeastward, the hurricane influence gradually diminishes and the overall upper ocean circulation returns approximately to the pre-storm pattern (not shown). Before Leslie approached, the upper-layer circulation in the inner bay features inflow and eddies (Fig. 7c). Six hours later when Leslie makes landfall on the western side of Placentia Bay, the upper-layer currents become stronger but remain inward. The different oceanic response is primarily attributed to differing hurricane tracks and landfall positions. Igor passes Placentia Bay on its eastern side making landfall 100 km away from Placentia Bay (Fig. 1). The dominant northwesty winds over Placentia Bay induce outward surface currents. In contrast, Leslie is on the western side of Placentia Bay. During the early stages of Leslie, the dominant southeastly winds induce inward surface currents.

4.2. Importance of local forcing in generating peak storm surge

Han et al. (2012b) and Ma et al. (2015) found the importance of remote oceanic forcing in generating the peak strong storm surge in Argentia during Igor. Here, we extend their studies to investigate the importance of local and remote forcing in storm surges during Igor and Leslie by carrying out sensitivity runs with the wind and air pressure turned off for the entire simulation period. The results are shown in Fig. 4, with detailed statistics in Table 5. During Igor, there are two surges at Argentia and St. Lawrence. The sensitivity run significantly underestimates the first one generated by local wind and air pressure when Igor makes landfall. In contrast, the sensitivity run captures the magnitude of the second (main) surge, similar to the baseline case. These results indicate that the second (main) surge is not generated by local winds or air pressure, consistent with previous observational and numerical studies by Han et al. (2012b) and Ma et al. (2015). They showed that the main surge is associated with the free propagating continental shelf wave. During Leslie, the main surge from the sensitivity run is under-estimated by 34% and 62% at Argentia and St. Lawrence when Leslie makes landfall (Table 5). Therefore, the effects of local wind and air pressure are significant in generating the peak surges during Leslie.

4.3. Near-inertial oscillation and its horizontal distribution

We also calculate the near-inertial speed (NIS) ($\sqrt{u^2 + v^2}$) near surface for Hurricane Igor (Fig. 8) and Leslie (Fig. 9). In order to extract velocity at the near-inertial frequency, a bandpass filter centred at 16 h is used. Snapshots are selected at peak of each NIS period, with the exact time marked in Fig. 5(c) and (g) by black dashed lines. The NIS is weak in the inner bay during both Igor (Fig. 8) and Leslie (Fig. 9). It is much stronger in the outer bay during Leslie than Igor, which can be attributed to the fact that the outer Placentia Bay is on the right side of Leslie and within the radius of the maximum winds but on the left side of Igor and outside of the radius of the maximum winds. During Igor, the NIS reaches maximum at landfall and decays rapidly afterwards (Fig. 8). During Leslie, the NIS reaches maximum (0.8 m s^{-1}) after landfall and dis-
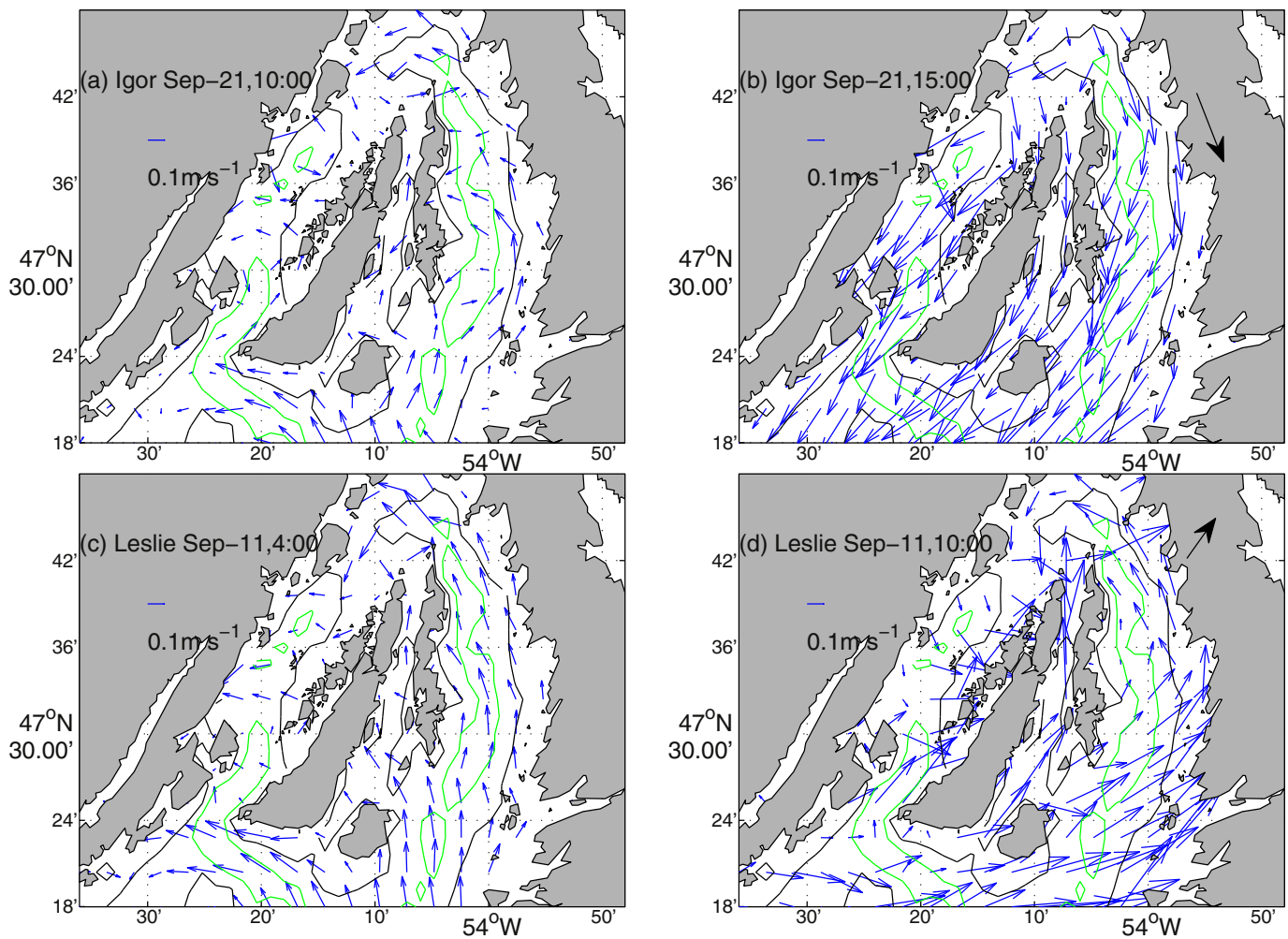
Fig. 7. 0–30 m averaged current under Igor and Leslie. Black arrows in (b) and (d) denote the relative magnitude and direction of wind averaged over the inner bay. (For interpretation of the references to color in the figure legend, the reader is referred to the web version of this article).

Table 5
Simulated storm surge at tide-gauge stations in the sensitivity case without local wind and air pressure.

Tide gauge station	Hurricane Igor		Hurricane Leslie	
	Argentia	St. Lawrence	Argentia	St. Lawrence
Simulated surge (m)	0.79	0.68	0.93	0.98
Difference relative to the baseline case (%)	−18	−20	−34	−62

sipates relatively slowly (Fig. 9c and d). The NIS can decay with the dissipations to higher frequency oscillations (Pollard, 1980) or the dispersions to depths by the baroclinic waves (Gill, 1984). There is no obvious horizontal propagation of near-inertial oscillation for both hurricanes.

4.4. The importance of stratification in near-inertial oscillation

To examine the influence of stratification on oceanic responses to hurricanes, a homogeneous barotropic case (hereafter referred to as BT) was run for the domain of Placentia Bay. This case is initialized with the same velocity fields as for the baseline baroclinic case (referred to as BC). In BT, the model is run with spatially uniform temperature and salinity over the domain. Same wind and pressure forcing of BC (but without heat flux) is applied at the surface and the open boundaries in BT. River volume flux is applied but thermal and haline fluxes are not. The 0–30 m averaged current from BT (not shown here) have similar same circulation pattern to that from BC, but with smaller velocity magni-

tude and shorter time for near-inertial energy to dissipate. To further examine the baroclinic influence, we select M2 and M3 near-surface currents as example (Fig. 10). Obviously, currents in the BC case are much stronger than those in the BT case, not only where hurricane-induced near-inertia oscillation is weak (M2), but also where hurricane-induced near-inertia oscillation is strong (M3). The above comparison indicates that stratification is a key dynamic factor affecting near surface current and near-inertial oscillation during Igor and Leslie, consistent with Csanady (1972), Krajcar and Orlic (1995) and Chen and Xie (1997). To demonstrate the baroclinic effect on the vertical structure of currents, we examine the vertical profiles of currents from the BC and BT cases at M2 and M3 (Fig. 11). Two vertical profiles are shown at the times indicated in Fig. 10(c) and (g). Again, we clearly see the model current from the BT case is significantly weaker than that from the BC case during the hurricanes. The BC case shows strong increase of the current gradient in the vertical, as the first baroclinic mode in response to the hurricane forcing; while the BT case does not.
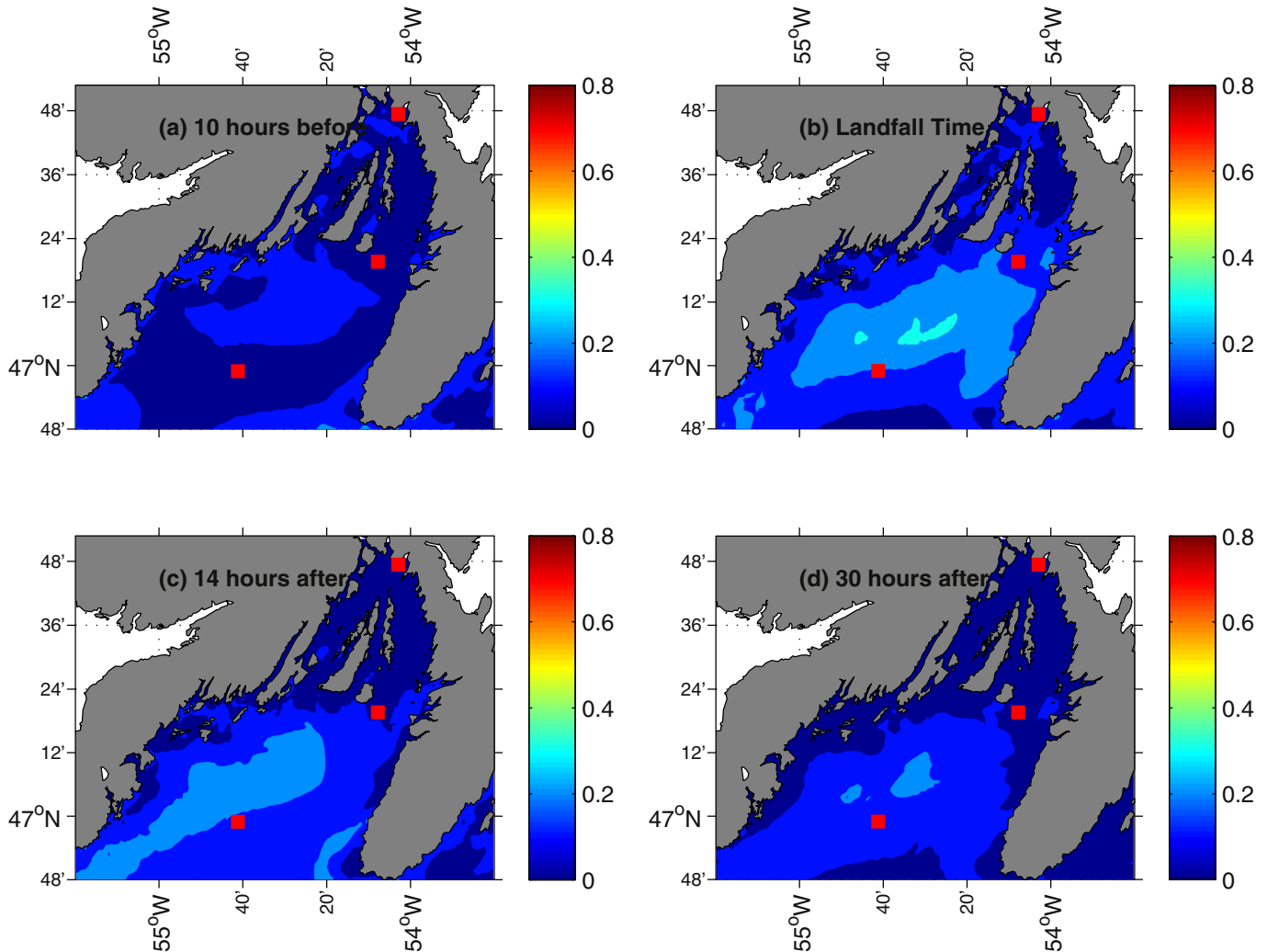
Fig. 8. Temporal evolution of the near-inertia speed at the sea surface (unit: m s^{-1}) during Hurricane Igor. Times for each panel are relative to the landfall time and marked in Fig. 5(c). (For interpretation of the references to color in the figure legend, the reader is referred to the web version of this article).

4.5. Evolution of temperature and salinity

To investigate the different responses of NIS under Igor and Leslie, the temporal evolution of temperature and salinity at M3 and its NIS are examined (Fig. 12). The near surface NIS is depicted as black line in Fig. 12 to represent NIS in the mixed layer before and after hurricanes. It should be noted that thermal effect contributes more to isopycnal distribution than haline effect at this location and thus we focus on thermocline variations. It is seen that a deep and thick thermocline layer exists before Igor, while this layer before Leslie is shallow and thin. Therefore, the stratification is stronger before Leslie than before Igor. The strong stratification before Leslie would prohibit the penetration of NIS from the mixed layer to the deep ocean, leading to strong NIS (black line in Fig. 12). As hurricanes make landfall, turbulent mixing is intensified, with decreasing of stratification and uplifting of thermocline. After wind resides, variations of the base of the mixed layer evolve towards equilibrium. This geostrophic adjustment leads to vertical displacement of thermocline, generation of near-inertial wave and internal wave. As seen in Fig. 12, strong turbulent mixing induced on the right side of Leslie generates larger vertical movement of the thermocline and thus contributes to stronger NIS inside the mixed layer. These results are consistent with the oceanic behavior in the wakes of storms from a linear theoretical simu-

lation (Gill, 1984) and the results of model departure mechanism (Zervakis and Levine, 1995).

4.6. Other important aspects affecting the model performance

Our modelling work indicates the critical importance of the quality of atmospheric forcing in achieving good model-observation agreement. When the NARR forcing field was used initially, the model underestimated the sea surface cooling and the mixed layer depth. We then reconstruct wind field and air pressure fields by blending the wind data at local weather stations and buoys. We also calculate net longwave, latent and sensible fluxes based on observations at weather station Argentia. The use of the reconstructed wind and pressure fields as well as the net longwave, latent and sensible heat fluxes at Argentia is a key aspect to achieve good model-observation agreement in the present study.

At the open boundary, our FVCOM implementation applies a relaxation scheme for temperature and salinity. Therefore it is important to use an appropriate relaxation time scale. In our case of simulating the responses of the mid-latitude ocean to hurricanes, we choose the time scale to be 24 h, a little longer than the local inertial period. An overly short time scale defeats the purpose of the relaxation scheme; while an overly long time scale significantly
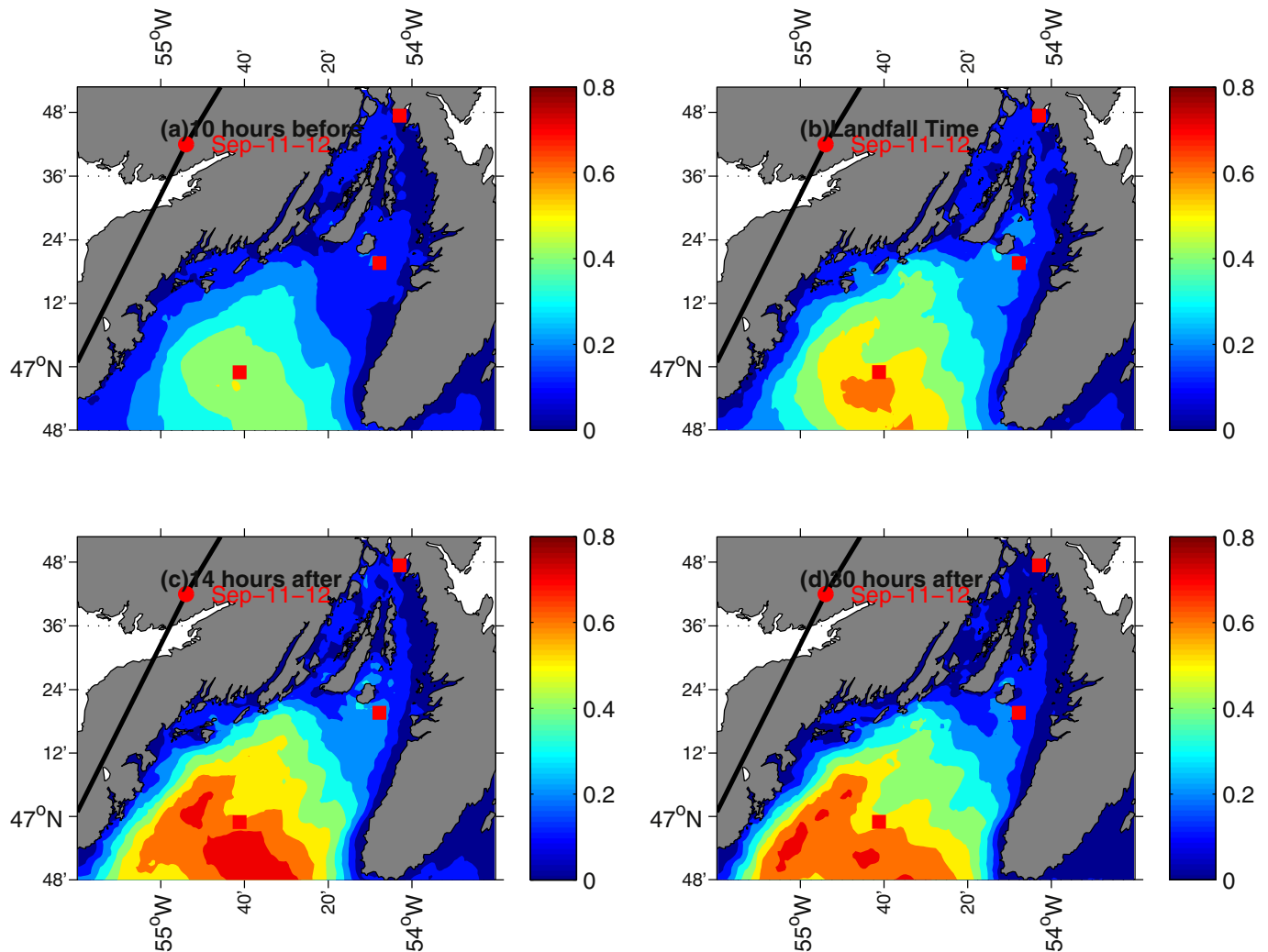
Fig. 9. Temporal evolution of the near-inertia speed at the sea surface (unit: m s^{-1}) during Hurricane Leslie. Times for each panel are relative to the landfall time and labeled at Fig. 5(g). (For interpretation of the references to color in the figure legend, the reader is referred to the web version of this article).

damps the effect of the boundary-imposed storm-scale variability inside the model domain.

In the present model a sigma-coordinate is used in the vertical. Since Placentia Bay has narrow and deep channels with a maximum model depth of 410 m, it is important to use high enough vertical resolution near the sea surface so that the dynamic and thermodynamic processes in the surface boundary layer can be resolved sufficiently. In the present model, the top layer has a maximum spacing of 0.9 m, and all the grid points for the top layer is within 0.45 m from the sea surface.

5. Conclusion

A three-dimensional finite-volume ocean model was applied to study the upper-layer ocean responses to two hurricanes in Placentia Bay, Newfoundland. The hurricanes chosen for the study are Hurricane Igor (2010) and Hurricane Leslie (2012). Hurricane Igor was the most powerful storm, making landfall on the eastern side of bay while Hurricane Leslie made landfall at the western side. The two hurricanes feature different tracks, strength, and translation speed, resulting in quite different oceanic responses on sea level and upper-layer circulation.

The finite-volume ocean model well reproduced the water level rise before and after hurricanes. Especially, the surges generated by the passage of Hurricane Igor were well captured. The model near-surface current was compared with observations at three different locations in Placentia Bay, two of which were located at the inner bay. The statistics indicate reasonable agreement with observation. Especially during hurricane events, simulated currents well capture the observed currents as well as the near-inertial currents, in terms of magnitude and variability.

The model reproduced the general cyclonic circulation in Placentia Bay before the two hurricanes. The upper 30 m circulation responding to the two hurricanes had opposite patterns during landfall, strong outflow during Igor but strong inflow during Leslie. Cases without local wind and air pressure forcing were examined. The model results during Leslie showed the local forcing contributed to 34% and 62% of the peak storm surge magnitude at Argentia and St. Lawrence respectively. There were two surges during Igor and the second (main) surge was due to remote oceanic forcing entering through the upstream eastern open boundary.

Model circulation with and without stratification revealed the importance of baroclinicity for the near-surface currents and the near-inertial oscillation in Placentia Bay. The near surface currents and near-inertial oscillation during the two hurricanes were significantly weaker without stratification. Thus, the baroclinic effect was essential in reproducing the hurricane-induced current intensification and near-inertial oscillation in Placentia Bay. Ver-
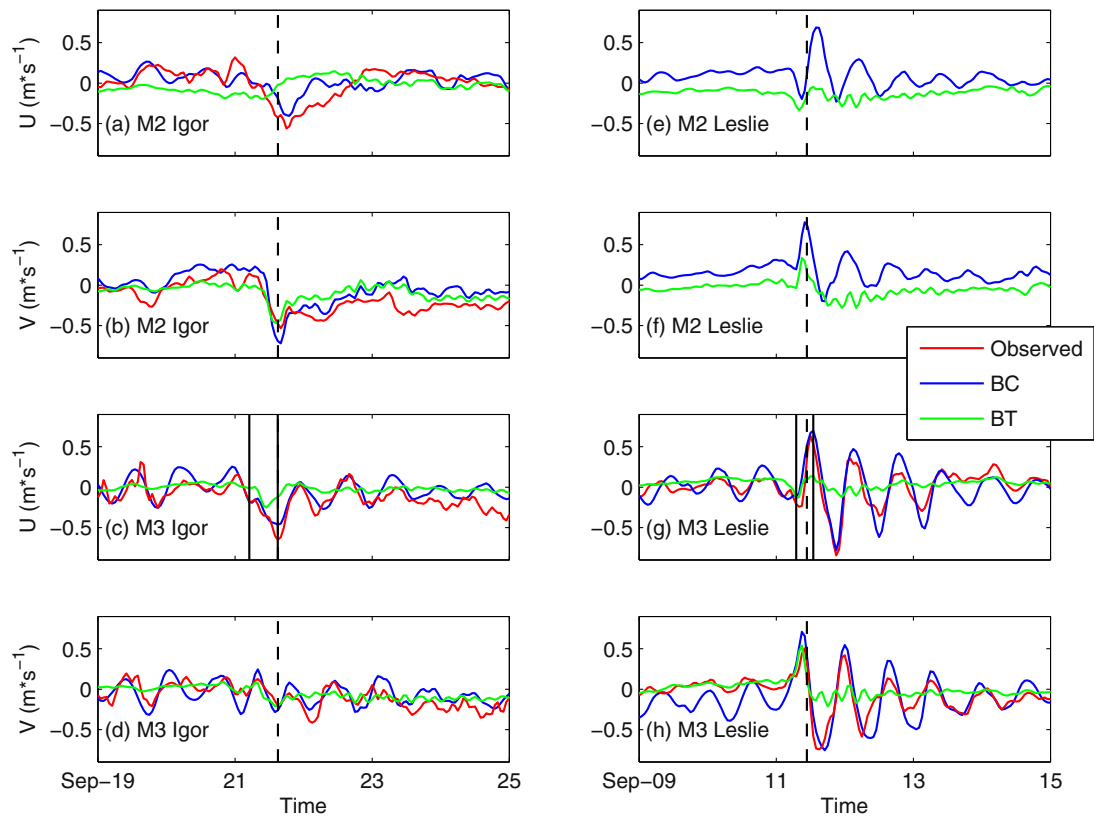
Fig. 10. Time series of near surface currents for case-BC and case-BT compared to the observed near surface currents (Red). Black dashed line indicates the landfall time at 15:00 21 September 2010 and 10:45 11 September 2012 for Igor and Leslie, respectively. Black thick lines at (c) and (g) are time of vertical current profiles for Fig. 11. (For interpretation of the references to colour in this figure legend, the reader is referred to the web version of this article.)
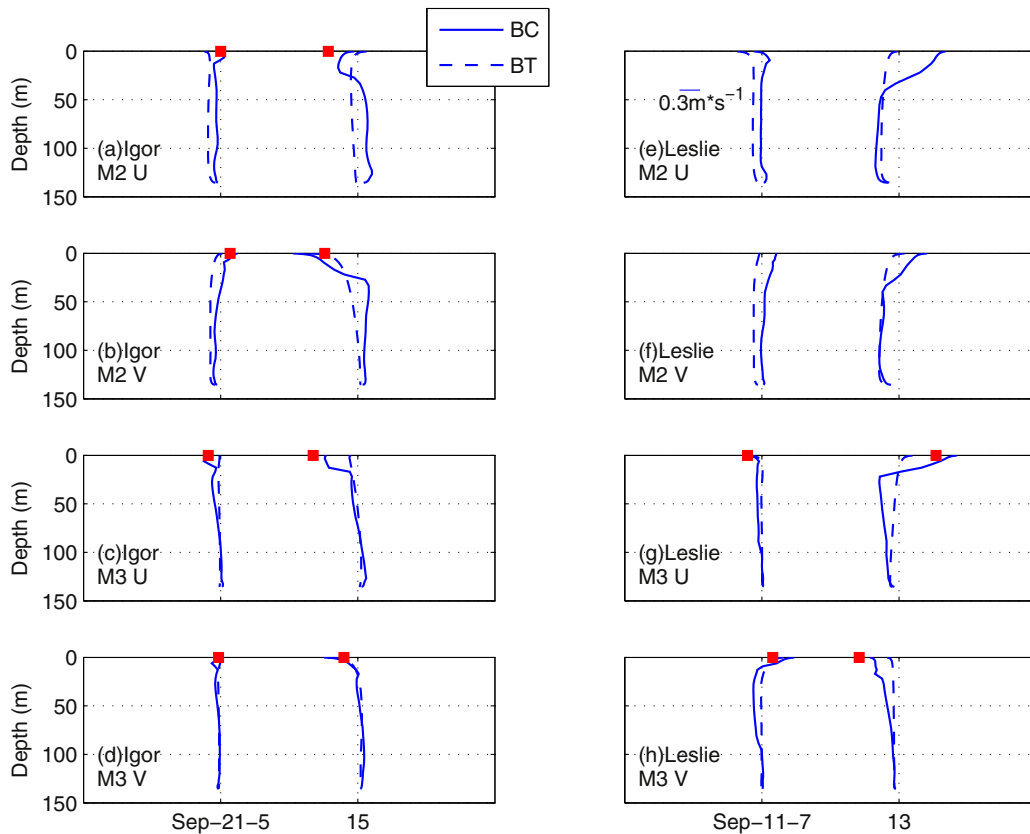
Fig. 11. Vertical profiles of currents at M2 and M3 under Hurricane Igor and Leslie. U is the eastward component and V is the northward component. Red squares indicate the observed near surface currents. X-axis indicates the time of each profile that labeled at Fig. 10(c) and (g). (For interpretation of the references to colour in this figure legend, the reader is referred to the web version of this article.)
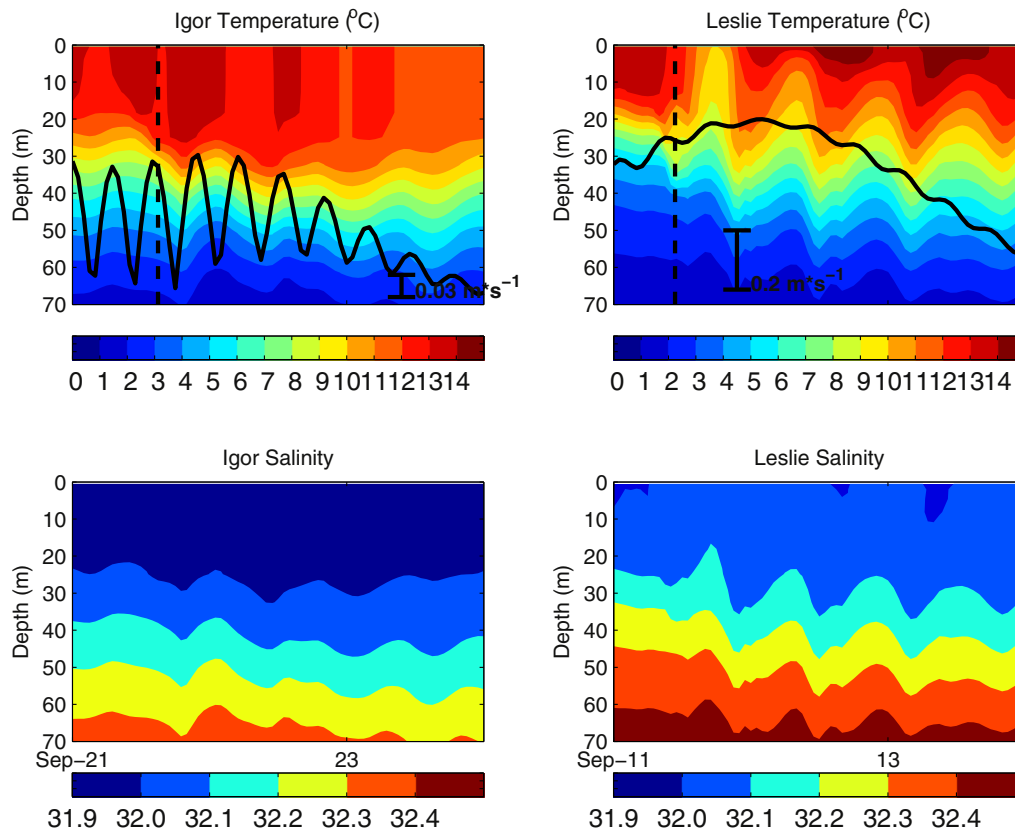
Fig. 12. Temporal evolution of temperature and salinity during Igor and Leslie. Black line indicates near surface near-inertial speed. (For interpretation of the references to color in the figure legend, the reader is referred to the web version of this article).

tical structures of the model currents at the mooring stations show substantially different vertical energy distributions between the baroclinic and barotropic cases. A strong pre-storm stratification during Leslie favours the generation of near-inertia oscillation. Strong turbulent mixing induced on the right side of Leslie generates large vertical movement of the thermocline and thus contributes to strong near-inertia oscillation inside the mixed layer. The barotropic simulation results in a significant underestimation of near-surface currents and near-inertial oscillation. The baroclinic simulation shows a large increase of the current gradient in the vertical, as the first baroclinic mode in response to the hurricane forcing.

Future improvements could be made to include two-way atmospheric-ocean coupling with the oceanic feedback on the hurricane latent heat flux (Bender and Ginis, 2000). The advantage of two-way coupling is to include the positive or negative feedbacks from ocean to the hurricane systems. For our study, the hurricane forcing is blended with observed data from local weather stations. The feedback from hurricanes to ocean has to some degree been accounted for through hourly wind speed, direction and air pressure.

Colorado, USA, from their Web site at http://www.esrl.noaa.gov/psd/.

References

Bender, M., Gins, I., 2000. Real-case simulations of Hurricane-Ocean interaction using a high-resolution coupled model; effects on hurricane intensity. Monthly Weather Rev 128, 917–946.

Bradbury, I.R., Snelgrove, P.V.R., Fraser, S., 2000. Transport and development of eggs and larvae of Atlantic cod, Gadus morhua, in relation to spawning time and location in coastal Newfoundland. Can. J. Fish. Aquat. Sci. 57, 1761–1772.

Csanady, G.T., 1972. Response of large stratified lakes to wind. J. Phys. Oceanogr. 2, 3–13.

Chen, C., Cowles, G., Beardsley, R.C., 2004. An unstructured grid, finite-volume coastal ocean model: FVCOM User Manual. SMAST/UMASSD Technical Report-04-0601. 183.

Chen, C., Xie, L., 1997. A numerical study of wind-induced, near-inertial oscillations over the Texas-Louisiana shelf. J. Geophys. Res. 102, 15583–15593.

Foreman, M., Czajko, P., Stucchi, D.J., Guo, M., 2009. A finite volume model simulation for the Broughton Archipelago, Canada. Ocean Modell. 30, 29–47.

Gill, A.E., 1984. On the behaviour of internal waves in the wakes of storms. J. Phys. Oceanogr. 14, 1129–1151.

Greenberg, D.A., Petrie, B.D., 1988. The mean barotropic circulation on the Newfoundland shelf and slope. J. Geophys. Res. 93, 15541–15550.

Greatbatch, R.J., 1983. On the response of the ocean to a moving storm: the nonlinear dynamics. J. Geophys. Res. 13, 357–367.

Han, G., 2005. Wind-driven barotropic circulation off Newfoundland and Labrador. Cont. Shelf Res. 25, 2084–2106.

Han, G., Lu, Z., Wang, Z., Helbig, J., Chen, N., deYoung, B., 2008. Seasonal variability of the Labrador Current and shelf circulation off Newfoundland. J. Geophys. Res. 113, 1–23.

Han, G., Ma, Z., de Young, B., Foreman, M., Chen, N., 2011. Simulation of three-dimensional circulation and hydrography over the Grand Banks of Newfoundland. Ocean Modelling 40, 199–210.

Han, G., Ma, Z., Chen, N., 2012a. Hurricane Igor impacts on the stratification and phytoplankton bloom over the Grand Banks. J. Mar. Syst. 100-101, 19–25.

Han, G, Ma, Z, Chen, D., deYoung, B., Chen, N., 2012b. Observing storm surges from space: Hurricane Igor off Newfoundland. Sci. Rep. 2, 1010. doi:10.1038/srep010101.

Hart, D.J., deYoung, B., Foley, J., 1999. Observations of currents, temperature and salinity in Placentia Bay, Newfoundland. Physics and Physical Oceanography Data Report 1998–9, Memorial University of Newfoundland, St. John's: Newfoundland.

Holland, G.J., 1980. An analytic model of the wind and pressure profiles in hurricanes. Mon, Weather Rev 108, 212–1218.

Krajcar, V., Orlic, M., 1995. Seasonal variability of inertial oscillations in the Northern Adriatic. Cont. Shelf. Res. 15, 1221–1233.

Kundu, P.K., 1976. An analysis of inertial oscillation observed near Oregon coast. J. Phys. Oceanogr. 6, 879–893.

Ma, Z., Han, G., deYoung, B., 2012. Modelling temperature, currents and stratification in Placentia Bay. J. Atmos. Ocean. 50, 244–260.

Ma, Z., Han, G., deYoung, B., 2015. Oceanic responses to hurricane Igor over the Grand Banks: a modelling study. J. Geophys. Res. Oceans 120. doi:10.1002/2014JC010322.

Mayer, D.A., Mofjeld, H.O., Leaman, K.D., 1981. Near-inertial waves observed on the outer shelf in the Middle Atlantic Bight in the wake of hurricane Belle. J. Phys. Oceanogr. 11, 87–106.

Mellor, G.L., Ezer, T., Oey, L.Y., 1993. The pressure gradient conundrum of sigma coordinate ocean models. J. Atmos. Ocean. Technol. 11, 1126–1134.

Mesinger, F., Dimego, G., Kalnay, E., Shafran, P., Ebisuzaki, W., Jovic, D., Wollen, J., Mitchell, K., Rogers, E., Fan, M., Ek, Y., Grumbine, R., Higgins, W., Li, H., Lin, Y., Manikin, G., Parrish, D., Shi, W., 2006. North American regional reanalysis. Bull. Amer. Meteorl. Soc. 87, 343–360.

Pasch, R.J., Kimberlain, T.B, 2011. Tropical Cyclone Report Hurricane Igor (AL112010).

Pawlowicz, R., Beardsley, B., Lentz, S., 2002. Classical tidal harmonic analysis including error estimates in MATLAB using T_TIDE. Comput. Geosci. 28, 929–937.

Perkins, H., 1976. Observed effect of an eddy on inertial oscillations. Deep-Sea Res 23, 1037–1042.

Pollard, R.T., 1980. Properties of near-surface inertial oscillations. J. Phys. Oceanogr. 10, 385–398.

Price, J.F., 1981. On the upper ocean response to a moving hurricane. J. Phys. Oceanogr. 11, 153–175.

Rabinovich, A., 2009. Seiches and harbour oscillations. In: Kim, Y (Ed.), Handbook of Coastal and Ocean Engineering. World Scientific Publ., Singapore 2009.

Rego, J.L., Li., C., 2010. Storm surge propagation in Galveston Bay during Hurricane Ike. J. Mar. Syst. 82, 265–279.

Resio, D.T., Westerink, J.J., 2008. Modeling the physics of storm surges. Phys. Today 61 (9), 33–38.

Shillinger, D.J., Simmons, P., deYoung, B., 2000. Analysis of the mean circulation in Placentia Bay: spring and summer 1999. Physics and physical oceanography data report 2000-1, Memorial University of Newfoundland: St. Johns, Newfoundland.

Shen, J., Gong, W., Wang, H., 2006. Water level response to 1999 Hurricane Floyd in the Chesapeake Bay. Cont. Shelf Res. 26, 2484–2502.

Tang, C.L., Gui, Q., Peterson, I.K., 1996. Modelling the mean circulation of the Labrador Sea and adjacent shelves. J. Phys. Oceanogr. 26, 1989–2010.

Weisberg, R.H., Zheng, L., 2006. Circulation of Tampa Bay driven by buoyancy, tides and winds, as simulated using a Finite Volume Coastal Ocean Model. J. Geophys. Res. 111, C1005. doi:10.1029/2005JC003067.

Zervakis, V., Levine, M.D., 1995. Near-inertial energy propagation from the mixed layer: theoretical considerations. J. Phys. Oceanogr. 25, 2872–2889.